The Manganese Salt (MnJ) Functions as A Potent Universal Adjuvant

Rui Zhang[1, 2, 6], Chenguang Wang[1, 2, 6], Yukun Guan[1, 2, 5, 6], Xiaoming Wei[1, 2], Mengyin Sha[1, 2], Miao Jing[1, 2], Mengze Lv[1, 2], Jing Xu[3], Yi Wan[4], Zhengfan Jiang[1, 2*]

[1]Key Laboratory of Cell Proliferation and Differentiation of the Ministry of Education, School of Life Sciences, Peking University, Beijing 100871, China

[2]Peking-Tsinghua Center for Life Sciences, Peking University, Beijing 100871, China

[3]CAS Key Laboratory for Biomedical Effects of Nanomaterials and Nanosafety, National Center for Nanoscience and Technology of China, Beijing 100190, China

[4]Laboratory for Earth Surface Processes, College of Urban and Environmental Sciences, Peking University, Beijing 100871, China

[5]Present address: Experimental Immunology Branch, National Cancer Institute, National Institutes of Health, Bethesda, Maryland, USA

[6]These authors contributed equally

*Correspondence: jiangzf@pku.edu.cn

Abstract:

Aluminum adjuvants have been used for a century in various vaccines due to its ability to potentiate humoral immunity and safety records since 1920s. Manganese is an essential micronutrient required for diverse biological activities in cells. We previously found that Mn^{2+} is a strong type I-interferon stimulator activating the cGAS-STING pathway. Herein we report that a colloidal manganese salt (MnJ) is a potent adjuvant to induce both humoral and cellular immune responses, particularly CTL activation. When administrated intranasally, MnJ was also a strong mucosal adjuvant, inducing high levels of IgA antibodies. MnJ strongly promoted dendritic cell maturation and antigen-specific T cell activation. Interestingly, IL-1/-18 induction and release by Mn^{2+}-activated ASC-mediated inflammasomes were not observed. MnJ showed great adjuvant effects to all tested antigens including inactivated viruses, recombinant proteins and peptides by either intramuscular or intranasal immunization. These findings may have implications in developing potent but safe Mn^{2+}-containing vaccines.

Main Text:

Vaccination is one of the most successful public health interventions. Adjuvants are widely used to increase the immunogenicity of vaccines with various advantages: (1) reducing the amount of antigens; (2) reducing the number of immunizations; (3) inducing a faster protection; (4) improving the efficacy of vaccines in newborns, the elderly or immunocompromised populations [1,2]. Over the past few decades, large amounts of adjuvants have been developed. According to their different mechanisms of action, adjuvants are divided into two categories: immune potentiators and

delivery systems. Some immune potentiators, composed of pathogen-associated molecular patterns (PAMPs) or synthesized activators of pattern-recognition receptors (PPRs), activate innate immune responses to induce the subsequent production of cytokines and chemokines. Other potentiators, composed of cells or cytokines like dendritic cells, IL-12 or GM-CSF, directly activate immunity. Delivery systems including liposome, micelles, virosome, nanoparticles, microsphere, Oil/Water emulsion, virus-like particles (VLP) and immune stimulating complexes (ISCOM), usually carry antigen to target cells and assist antigen uptake by antigen presenting cells (APCs) [3,4].

The immune enhancement effect of aluminum salts (Alum) was first reported by Glenny et al. in the 1920's when they found that injection of guinea pigs with diphtheria toxoid precipitated with potassium aluminum provided greater protection than toxoid alone [5]. Since then, Alum-containing adjuvants have been employed in billions of doses of vaccines and administered annually to millions of people [6]. In fact, Alum is the only human adjuvant widely used, partly due to its minimal reactogenicity and inexpensiveness [7]. However, Alum-adjuvanted vaccines need repeated administrations which may cause or manifest its adverse effects including increased IgE production and neurotoxicity [8]. In addition, Alum mainly induces T helper 2 (TH2) cell response through NLPR3 inflammasome activation [9-11], but not TH1 or cytotoxic T-lymphocyte (CTL) response [1,12]. Therefore, Alum is generally believed to be unable to elicit cellular immune responses that are essential for virus or tumor vaccines.

In the past decades, however, the medical need for new adjuvants is increasing as (1) the tremendously increased use of purified antigens like recombinant proteins with low

55 immunogenicity due to the absence of immunostimulatory components recognized by PRRs; (2)
56 adjuvants inducing cellular immune responses especially CTL are badly needed for virus and
57 cancer vaccines [13-15]. So far few adjuvants have been approved by the US Food and Drug
58 Administration for use in humans and several formulations are in clinical trials. The oil-in-water
59 MF59 in influenza vaccines for the elderly was approved in the 1990's, followed by AS03 in
60 vaccines against avian influenza virus, AS04 in hepatitis B virus (HBV) and human papillomavirus
61 (HPV) vaccines, and AS01 in herpes zoster virus vaccines [16]. Toll-like receptor (TLR) agonists,
62 like the CpG DNA and poly (I:C), have been studied in the past two decades as new adjuvant
63 candidates [7]. cGAS-STING [17-20] agonists like DMXAA [21], c-di-GMP [22], cGAMP [23] and Chitosan [24]
64 also showed some adjuvant effects.

65 Manganese (Mn) is a nutritional inorganic trace element required for a variety of physiological
66 processes including development, reproduction, neuronal function and antioxidant defenses [25,26].
67 Mn (Mn^{2+} in general cases) is essential for some metalloenzymes such as Mn superoxide dismutase
68 (SOD2, Mn^{3+} or Mn^{2+} in this case), glutamine synthetase (GS), and arginase [27]. However, its
69 function in regulating immunity is largely unknown. Previously we found that Mn^{2+} was required
70 for the host defense against DNA virus by increasing the sensitivity of the DNA sensor cGAS and
71 its downstream adaptor protein STING. Mn^{2+} was released from mitochondria and Golgi apparatus
72 upon virus infection and accumulated in the cytosol where it bound directly to cGAS, enhancing
73 the sensitivity of cGAS to double-stranded DNA (dsDNA) and its enzymatic activity. Mn^{2+} also
74 enhanced cGAMP-STING binding affinity [28]. Importantly, Mn^{2+} was a potent innate immune
75 stimulator, inducing type I-IFN and cytokine production in the absence of any infection.

Herein we report that Manganese (Mn^{2+}) functions as a universal non-inflammatory adjuvant to induce both humoral and cellular immune responses, particularly CTL activation. A colloidal manganese salt (MnJ) was found to strongly promote dendritic cell maturation and antigen-specific T cell activation. When administrated intranasally, MnJ was also a strong mucosal adjuvant, inducing high levels of IgA antibodies. MnJ showed great adjuvant effects to all tested antigens including inactivated viruses, recombinant proteins and peptides by either intramuscular or intranasal immunization. Thus, we identified the second metal element that functions as adjuvant nearly one hundred years after Alum was found.

Results:

Mn^{2+} Promotes DC Maturation via cGAS-STING Activation

We previously found that Mn^{2+} is a strong type I-IFN stimulator by activating the cGAS-STING pathway in the absence of any infections *in vitro* and *in vivo*, we thus hypothesized that Mn^{2+} would have some adjuvant potentials. Since APCs play an important role in linking innate and adaptive immunity, we first determined whether Mn^{2+} promotes DC maturation. RNA-seq analysis on Mn^{2+}- or LPS-treated mouse bone marrow derived dendritic cells (BMDCs) revealed that Mn^{2+} induced robust production of both IFNβ and various IFNαs, which were not induced by LPS (Fig. 1a), together with significantly up-regulated costimulatory molecules CD80 and CD86, mouse MHC-I proteins H-2K/D/Q, immunoproteasome subunits PSMB8/9, peptide transporters TAP1/2 and chemokines, including CCL2 and CCL3, that increase the recruitment of immune cells to the injection site. Surprisingly, compared to LPS-treated BMDCs, Mn^{2+}-treated BMDCs did not

96 produce pro-inflammatory cytokines including IL-1α/β and IL-18, nor IL-10 or IL-12, suggesting
97 that Mn^{2+} triggered a distinct signaling in BMDCs, which were confirmed by qPCR analysis (Fig.
98 1b). Additionally, Mn^{2+}-induced expression of costimulatory molecules CD86, CD80 and CD40
99 were lost in BMDCs from *Tmem173*$^{-/-}$, *Irf3*$^{-/-}$*Irf7*$^{-/-}$ and *Ifnar*$^{-/-}$ mice, showing that Mn^{2+}-induced
100 DC maturation was completely dependent on the activation of the cGAS-STING pathway (Fig.
101 1c).

102 **Mn^{2+} Activates NLRP3 Inflammasome**

103 Alum has been shown to activate the NLRP3 inflammasome and the capacity of Alum to promote
104 antibody production was compromised in *Caspase1*$^{-/-}$, *Pycard*$^{-/-}$ or *Nlrp3*$^{-/-}$ mice [9-11]. To compare
105 the ability of Mn^{2+} and Aluminium-containing adjuvants (Imject® Alum, Alhydrogel® adjuvant
106 and Adju-Phos® adjuvant) to activate innate immunity, we tested the production of type I-IFNs and
107 pro-inflammatory cytokines IL-1β and IL-18 in peritoneal macrophages treated with Mn^{2+} or
108 various Alums. Only Mn^{2+} induced type I-IFNs (Fig. 2a). Mn^{2+} also activated stronger
109 inflammasome than Imject® Alum and Alhydrogel® Alum did (Fig. 2b, c), which was entirely
110 dependent on ASC, mainly on NLRP3 (Fig. 2d-g). Interestingly, Mn^{2+}-induced inflammasome
111 activation in mouse cells was different from THP1 cells, which showed a complete
112 NLRP3-dependence (Fig. 2h, Extended Data Fig. 1a). Moreover, cGAS or STING deficiency did
113 not affect Mn^{2+}-activated inflammasome in macrophages from *Cgas*$^{-/-}$, *Tmem173*$^{-/-}$ mice or
114 *CGAS*$^{-/-}$, *TMEM173*$^{-/-}$ THP1 cells (Extended Data Fig. 1b-e), indicating that cGAS-STING
115 -induced lysosomal cell death [29], or cGAMP production [30] was not essential for Mn^{2+}-induced

inflammasome. Instead, we found that N-acetyl-L-cysteine (NAC, a direct scavenger of ROS), reduced L-glutathione (GSH, an intracellular thiol antioxidant), extracellular K^+, or 2-APB (a cytosolic Ca^{2+} release inhibitor) all restrained Mn^{2+}-induced inflammasome activation (Extended Data Fig. 2a-g). Using a modified culture medium, Hanks' Balanced Salt Solution Deletion of PO_4^{3-} and CO_3^{2-} (herein HBSSD), in which Mn^{2+} and Ca^{2+} did not form particles, we found that Mn^{2+} activated NLRP3 and pyroptosis were essentially independent of particle formation, which is different from Ca^{2+} (Extended Data Fig. 2h, i). mtDNA depletion (Extended Data Fig. 2j) by ethidium bromide [28] did not affect Mn^{2+}-induced inflammasome activation either (Extended Data Fig. 2k, l). We thus concluded that Mn^{2+} activated stronger NLRP3 inflammasome than Alum did.

Mn^{2+} Activates Inflammasome without IL-1/-18 Production

Consistent with results from RNA-seq and qPCR (Fig. 1a, b), Mn^{2+} treatment did not induce upregulation of *Il1b* and *Il18* in both murine BMDCs and human monocyte derived dendritic cells (Mo-DCs) (Fig. 3a). Interestingly, Alum activated NLRP3 inflammasome in a similar way, neither Mn^{2+} nor Alum induced IL-1/18 production without LPS priming (Fig. 3b, c). The same results were obtained when human peripheral blood mononuclear cells (PBMCs) were treated with Mn^{2+} (Fig. 3d). Since clinical studies on various inflammatory diseases suggested the crucial role for IL-1/-18 but not for TNFα, which only amplified and perpetuated the damage [31], we held that Mn^{2+}-activated inflammasome did not cause systematic inflammation but may still be critical for its adjuvant activity (see below).

MnJ Is A Potent Universal Adjuvant

Given that Mn^{2+} induced strong type I-IFN production and NLRP3 inflammasome activation, we reasoned that Mn^{2+} could be used as an adjuvant. To test this, we first immunized C57BL/6 mice with LPS-free chicken ovalbumin protein (OVA) alone or OVA with different Mn^{2+} solutions intramuscularly (i.m.) or intranasally (i.n.) and measured OVA-specific antibodies. Surprisingly, we found that only Mn^{2+} in phosphate buffer saline (PBS), but not Mn^{2+} in normal saline, promoted antibody production (Extended Data Fig. 3a, b). The difference was that Mn^{2+} formed particles in PBS but not in saline, suggesting that soluble Mn^{2+} was unable to induce a local immune response as expected. However, Mn^{2+} particles in PBS tended to aggregate and precipitate with time, thus lost its adjuvant activity (Extended Data Fig. 3c). By screening various manganese compounds, we generated jelly-like Mn^{2+} colloids (MnJ, Mn Jelly) (Extended Data Fig. 3d) consisting of elongate nanoparticles approximately 2 × 2 × 6 nm in size (Extended Data Fig. 3e). MnJ was stable without aggregation in the following experiments. Its adjuvant effect was not weakened after storage at -80 ℃ for three weeks or longer, or even after freeze–drying/lyophilization (Extended Data Fig. 3f). On the contrary, Alum vaccines are known to be sensitive to freezing and thus hard to store or transport. Interestingly, MnJ triggered comparable inflammasome activation (Extended Data Fig. 3g), but stronger type I-IFN production than $MnCl_2$ or Mn^{2+}-PBS did (Extended Data Fig. 3h), probably due to the facilitated transportation into cells as nanoparticles [32,33]. Compared to $MnCl_2$, which disappeared within hours, MnJ had a much longer muscle retention time up to 8 days at the site of injection, similar to Mn^{2+}-PBS particles (Extended Data Fig. 3i). Splenocytes were isolated from OVA-immunized mice and stimulated with major histocompatibility class II (MHC-II)-binding OVA peptide I-A^b and MHC-I-binding

157 peptide H-2K^{b} to compare T cell activation. IFNγ induced in splenocytes from OVA-MnJ was
158 higher than OVA-Mn^{2+} (Extended Data Fig. 3j). Consequently, the adjuvant effect of MnJ was
159 significantly better than that of Mn^{2+}-PBS (Extended Data Fig. 3a-c).

160 We next evaluated the detailed adjuvant effect of MnJ. MnJ-adjuvanted antibody induction by
161 intramuscularly immunization showed dose-dependence and lasted for at least 6 months (Fig. 4a).
162 Compared to three different Aluminum-containing adjuvants, MnJ induced much stronger
163 OVA-specific IgG1 production and CTL response (Fig. 4b). We also compared MnJ with other
164 adjuvants including the complete Freund's adjuvant (CFA), incomplete Freund's adjuvant (IFA),
165 MF59 and polyetherimide (PEI). We found that MnJ adjuvant effect was even better than CFA (20
166 μg MnJ vs 50 μl CFA, i.m.) and MF59 (20 μg MnJ vs 50 μl MF59, i.m.) (Extended Data Fig. 3k, l).
167 Also, MnJ boosted specific antibody production against different recombinant protein/peptide
168 antigens, including influenza A/PR8 hemagglutinin A1 peptide, haptenized experimental antigen
169 nitrophenol-conjugatd keyhole limpet hemocyanin (NP-KLH), HBV surface antigen (HBsAg) and
170 HBSS1 fusion protein (containing S (1-223 aa) and PreS1 (21-47 aa)) [34], and inactivated
171 enterovirus type 71 (EV71) (Fig. 4d). Besides, intranasally immunization revealed that MnJ was
172 also a potent mucosal adjuvant, inducing high levels of IgA antibodies in lung, saliva, and serum
173 for a long time and as good as cholera toxin B (5 μg MnJ vs 10 μg CTB, i.n.) [35] (Fig. 4e, f).

174 Importantly, compared to CFA-injected mice showing prominent swellings and granulomas with
175 one shoot (Extended Data Fig. 4a), MnJ-injected mice displayed no visible side effects on injection
176 site, body weight, survival or different organs even after repeated administrations (3 shoots in 3

consecutive weeks) (Extended Data Fig. 4a-i), suggesting that MnJ is a safe adjuvant with good biocompatibility.

MnJ Promotes Antigen Presentation and T Cell Responses

MF59 and Alum facilitate APCs to engulf antigens and transport them to draining lymph nodes (dLNs), and also induce the differentiation of monocytes to dendritic cells (Mo-DCs) [36,37]. So, we next evaluated antigen uptake by APCs and Mo-DC differentiation in dLNs after MnJ administration. We immunized mice in both inguinal regions subcutaneously with fluorescent protein Phycoerythrin (PE) containing MnJ or Alum adjuvant. APCs in inguinal lymph nodes were analyzed by flow cytometry afterwards. The percentage and number of PE-loaded APCs were significantly enhanced 12 and 24 h after MnJ immunization (Fig. 5a). Also, there was a significant increase in the accumulation of Mo-DCs in mice immunized with antigen plus MnJ compared to that in mice immunized with antigen alone (Fig. 5b).

The capacity of MnJ to promote BMDC maturation was stronger compared with Mn^{2+}, while Alum did not have any effect (Fig. 5c). *In vivo*, MnJ enhanced both $CD4^+$ and $CD8^+$ T cell proliferation, whereas Alum only induced a weak $CD4^+$ T cell proliferation (Fig. 5d). Splenocytes were next isolated from OVA-immunized mice and stimulated with OVA to compare T cell activation. IL-2 and IFNγ were highly induced in splenocytes from OVA-MnJ, but not OVA-Alum immunized mice, whereas IL-4 and IL-10 were preferably produced via OVA-Alum immunization (Fig. 5e), indicating that MnJ potently stimulated TH1 response, in addition to TH2 response. Accordingly, *in vivo* cytotoxic assay showed that MnJ immunized mice generated very strong CTL activities in

197 killing OVA-bearing cells, which was absent in Alum immunized mice (Fig. 5f). MnJ also
198 promoted the formation of germinal center (GC) with significantly increased amounts of Tfh and
199 GC B cells (Fig. 5g).

200 **Both cGAS-STING and NLRP3 Inflammasome Contribute to Adjuvant Activity of MnJ**

201 Next, *Tmem173*$^{-/-}$, *Mavs*$^{-/-}$, *Nlrp3*$^{-/-}$, *Nlrc4*$^{-/-}$, *Aim2*$^{-/-}$ or *Pycard*$^{-/-}$ mice were used to test which
202 pathway is involved in MnJ's adjuvant effect. It was found that although *Tmem173*$^{-/-}$, *Pycard*$^{-/-}$ or
203 *Nlrp3*$^{-/-}$ mice produced diminished OVA-specific antibodies (Extended Data Fig. 5a),
204 *Tmem173*$^{-/-}$*Pycard*$^{-/-}$ (double knockout, DKO) mice generated extremely decreased OVA-specific
205 antibodies (Fig. 6a-c), suggesting that both cGAS-STING and inflammasome contributed to MnJ
206 adjuvant effect. Further, *Tmem173*$^{-/-}$*Nlrp3*$^{-/-}$ mice generated a bit more antibodies than
207 *Tmem173*$^{-/-}$*Pycard*$^{-/-}$ mice did (Fig. 6a-b), indicating the involvement of other ASC-dependent
208 inflammasome activation by MnJ. We also analyzed the expression of *Dock2*, which was reported
209 to be down-regulated in *Pycard*$^{-/-}$ but not *Nlrp3*$^{-/-}$ or *Caspase1*$^{-/-}$ mice [38]. Quantitative PCR
210 analysis confirmed the same expression of *Dock2* mRNA in WT, *Tmem173*$^{-/-}$, *Pycard*$^{-/-}$, *Nlrp3*$^{-/-}$,
211 *Tmem173*$^{-/-}$*Pycard*$^{-/-}$ and *Tmem173*$^{-/-}$*Nlrp3*$^{-/-}$ mice (Extended Data Fig. 5b). Consistently,
212 MnJ-promoted germinal center formation was impaired in the DKO (specifically referred to
213 *Tmem173*$^{-/-}$*Pycard*$^{-/-}$ in the following text) mice (Extended Data Fig. 5c). In addition,
214 MnJ-induced OT-II CD4^{+} T cell proliferation disappeared in the DKO mice (Fig. 6d), along with
215 sharply reduced IFNγ and IL-2 production by peptide-stimulated splenic T cells (Fig. 6e).
216 Consistent with previous results (Fig. 3d, e), no IL-1β induction was detected in lymph nodes from

MnJ-treated mice *in vivo*, despite of ISG production and GSDMD cleavage (Fig. 6f). Since neither Mn^{2+} nor MnJ treatment did induce IL-1 or IL-18 expression *in vitro* or *in vivo*, we reasoned that ASC-mediated inflammasome activation contributed to MnJ adjuvant activity by releasing other DAMPs like uric acid [39], but not by IL-1 or TNFα, consistent with previous reports that neither of them was important for adjuvant effect [22,40]. However, CFA or Monophosphoryl Lipid A (MPLA) induced antibody production did not change much among these mice (Extended Data Fig. 5d, e).

MnJ Is A Potent Adjuvant for Antiviral and Antitumor Vaccines

Next we tested the protection effect of MnJ adjuvanted vaccines against various viruses. Formaldehyde-inactivated Vesicular stomatitis virus (VSV), Herpes simplex virus 1 (HSV-1) and Vaccinia Virus (VACV) were used as vaccines. The optimal dose for each inactivated virus was first determined (VSV and HSV i.m.; VACV i.n.) (Extended Data Fig. 6a-f). MnJ greatly enhanced the protection efficacy of inactivated virus by about 100 times, which is much better than Alum. Consistently, virus titers were decreased by at least 10^3 times in MnJ immunized mice (Fig. 7a-f), indicating that MnJ can be applied to all tested virus vaccines through either intramuscular or intranasal immunization, with greatly reduced amounts of inactivated-virus needed for an adequate protection.

We particularly tested MnJ in influenza vaccines. Mice immunized with virus protein HA1 (PR8) plus MnJ (i.m. or i.n.) or HA1 plus CTB (i.n.) were completely protected from lethal H1N1 A/PR8/34 virus challenge, while Alum adjuvant only showed mild protection (Fig. 7g, h, Extended Data Fig. 6g-i). Importantly, MnJ enhanced the protection effect of inactivated PR8 vaccine by at

237 least 10 times (Fig. 7i). Moreover, MnJ exhibited superior protection against heterologous
238 influenza viruses to mice immunized with MnJ-adjuvanted inactivated PR8 or HA1 protein,
239 followed by lethal H1N1 WSN or H3N2 challenge (Extended Data Fig. 6j).

240 Finally, the adjuvant effect of MnJ on cancer vaccines was evaluated. Mice were immunized three
241 times before inoculated with melanoma cell B16-OVA subcutaneously. Tumor growth was greatly
242 suppressed in OVA-MnJ, but not OVA-Alum, immunized mice (Fig. 7j, Extended Data Fig. 7a), in
243 line with prominently improved survival (Fig 7k) and increased tumor-infiltrating $CD4^+$ and $CD8^+$
244 T cells (Extended Data Fig. 7b, c), confirming CTL inducing activity of MnJ. In pulmonary
245 metastasis model, OVA-MnJ immunization greatly blocked lung metastases in the WT, but not
246 *Tmem173*$^{-/-}$*Pycard*$^{-/-}$ mice (Fig. 7l, m, Extended Data Fig. 7d), which is consistent with the
247 proliferation of $CD8^+$ OT-I T cells (Extended Data Fig. 7e). In addition, OVA-specific antibody
248 production and $CD8^+$ T cell activation analyzed by tetramer assays were only detected in
249 MnJ-OVA immunized WT mice (Fig. 7n, Extended Data Fig. 7f, g), suggesting its potentials in
250 tumor therapies.

251 **DISCUSSION**

252 The adjuvant activity of Aluminum was found by Alexander Glenny and his colleagues in 1926 [41],
253 now almost one century later, we reported the adjuvant activity of another metal-Manganese.
254 Adjuvant effect is essentially attributed by type I-IFN-promoted dendritic cell maturation and
255 migration to prime adaptive immune responses along with 1) local up-regulation of chemokines,
256 including CCL2 (MCP-1) and CCL3 (MIP-1α) to recruit immune cells to the injection site; 2)

increase of antigen uptake by immune cells; 3) induction of monocyte differentiation into dendritic cells [8,36,37]. We found that Mn^{2+} induced APCs to produce both IFNβ and various IFNαs, which were surprisingly not induced by LPS, together with many co-stimulatory and MHC molecules crucial for antigen presentation and chemokines for immune cell recruitment. MnJ also strongly enhanced antigen uptake by APCs and the differentiation of monocytes to dendritic cells. Importantly, Mn^{2+} did not induce the production of pro-inflammatory cytokines IL-1 and IL-18 in human or mouse *in vitro* and *in vivo*. Therefore, MnJ demonstrated superior adjuvant effects as it induces humoral, cellular, and mucosal immune responses, particularly CTL activation, without detected side-effects. In addition, the adjuvant effect of MnJ was stable even after repeated freeze-drying cycles, whereas Alum is sensitive to freezing and requires cold-chain temperature control [42,43]. MnJ showed great adjuvant effects to all tested vaccine antigens including inactivated viruses, recombinant protein subunits and peptides, thus it can significantly reduce the amount of viruses needed. Particularly, its tumor antigen-specific CTL activity by either intramuscular or intranasal MnJ immunization indicated a great potential for cancer vaccines. Based on these results, we believe that MnJ has great potentials for the development of potent but safe vaccines. The component simplicity and steadiness of MnJ, the low cost and wide availability of Mn make this adjuvant even more promising.

Although Alum adjuvanted vaccines have been proven to be safe in most cases, some studies showed that aluminum accumulation are associated with long-lasting macrophagic myofasciitis (MMF) [44], nervous disoders [45] and bone disease [46] in some patients. The FDA-approved doses of 850 μg, 1140 μg, and 1250 μg Alum per vaccine were determined according to antigenicity and

effectiveness of vaccine, not including safety consideration [47-49]. After vaccine injection, Alum has been found in the injected muscle, draining lymph nodes and spleen 9 months in humans [50] or even 12 years in patients with ASIA (Autoimmune/inflammatory syndrome induced by adjuvants) [51,52]. Consistently, we found that intramuscularly injected Alum in mice did not show obvious clearance 2 weeks after injection whereas injected MnJ was beyond detection after 8 days. Importantly, MnJ, but not Alum, could be readily decomposed into free Mn^{2+} ions by many common acidic metabolic products or under acidic environment (data not shown). In addition, tumor microenvironment is characterized by anomalous metabolic properties and acidic environment [53], which might be beneficial for the application of MnJ in antitumor therapy. Excessive Mn accumulation in the central nervous system causes neurologic toxicity in occupational cohorts through inhalation from welding or smelting [26]. However, we found that 20 μg MnJ induced higher antibody production than 1444 μg Imject® Alum, 1444 μg Alhydrogel® adjuvant 2%, 2259μg Adju-Phos® adjuvant (500 μg Alum in each) did, indicating MnJ is at least 25 times more potent than Alum in terms of inducing humoral immune response, which means that much smaller amount of MnJ can achieve the same effect.

There is still controversy about the function of NLRP3 inflammasome on adjuvant effect of aluminum salt [12]. These different conclusions may result from different aluminum salts or mice backgrounds used. There is also another view that ASC has an inflammasome-independent role in shaping adaptive immunity, for regulating the expression of Dock2, which is important for antigen uptake and lymphocyte mobility [38]. However, we found that STING, NLRP3 or ASC deficiency did not affect the expression of Dock2 in macrophages or lymphocytes. Interestingly, manganese

299 salts administration did not upregulate pro-IL-1β or pro-IL-18 production, which means that MnJ
300 activate adaptive immune responses partly through an inflammasome-dependent but inflammatory
301 cytokines-independent manner. In this regard, there may be some other stimulators upregulated by
302 MnJ and released by pyroptotic death of cells. However, even though we did not detect IL-1/-18
303 production by macrophages or PBMCs treated with $MnCl_2$ alone, these cells may generate these
304 cytokines when treated with inactivated pathogens plus $MnCl_2$. IL-1 and IL-18 can promote the
305 infiltration of neutrophils and enhance immune responses after immunization with adjuvants like
306 Alum or ISCOMATRIX [40,54,55].

307 In addition, similar to Alum adjuvant, the MnJ nanoparticles were also able to absorbe antigens
308 like OVA, GFP or PE proteins (data not shown). The physical depot effect of MnJ retained antigens
309 at the injection site and enhanced the uptake of antigens by APCs. Generally, MnJ is an adjuvant
310 owning the properties of both immune potentiator and delivery system. Because of its excellent
311 adjuvant activities and stability against repeated freezing-thaw treatment, Mn-based adjuvants
312 would be especially useful in veterinary vaccines with the following three additional advantages. 1)
313 MnJ showed a very nice dose-dependent adjuvant activity intramuscularly or intranasally, with 20
314 μg MnJ per mouse showing stronger antibody inducing activity than any tested adjuvants including
315 CFA; 2) High MnJ dose (up to several mg/shot) and repeated administrations to mice, rabbits or
316 pigs (data not shown) did not cause any visible damage or inflammation such as swellings and
317 granulomas at the injection sites or in various organs; 3) Mammals keep tissue Mn levels via tight
318 control of both absorption and excretion, as normally only 1–5% of ingested Mn is absorbed into
319 the body [56] and excessive dietary Mn causes reduced Mn absorption and enhanced Mn metabolism

and excretion [57-59]. Therefore, even highly elevated Mn levels in meats caused by Mn-containing veterinary vaccines would unlikely increase gastrointestinal Mn absorption by humans. In fact, Mn contents in whole grains, rice, and nuts are around or more than 30 mg Mn/kg or even 110-140 mg Mn/kg in wheat bran, much higher than those in mammals that are between 0.3 and 2.9 mg Mn/kg wet tissue weight, confirming the tight Mn absorption by animals.

References and Notes:

1 Petrovsky, N. & Aguilar, J. C. Vaccine adjuvants: current state and future trends. *Immunology and cell biology* **82**, 488-496, doi:10.1111/j.0818-9641.2004.01272.x (2004).

2 Apostolico Jde, S., Lunardelli, V. A., Coirada, F. C., Boscardin, S. B. & Rosa, D. S. Adjuvants: Classification, Modus Operandi, and Licensing. *Journal of immunology research* **2016**, 1459394, doi:10.1155/2016/1459394 (2016).

3 Pashine, A., Valiante, N. M. & Ulmer, J. B. Targeting the innate immune response with improved vaccine adjuvants. *Nature medicine* **11**, S63-68, doi:10.1038/nm1210 (2005).

4 Kaurav, M., Madan, J., Sudheesh, M. S. & Pandey, R. S. Combined adjuvant-delivery system for new generation vaccine antigens: alliance has its own advantage. *Artif Cells Nanomed Biotechnol* **46**, S818-S831, doi:10.1080/21691401.2018.1513941 (2018).

5 McKee, A. S. & Marrack, P. Old and new adjuvants. *Curr Opin Immunol* **47**, 44-51, doi:10.1016/j.coi.2017.06.005 (2017).

6 Clements, C. J. & Griffiths, E. The global impact of vaccines containing aluminium adjuvants. *Vaccine* **20 Suppl 3**, S24-33 (2002).

7 O'Hagan, D. T., Friedland, L. R., Hanon, E. & Didierlaurent, A. M. Towards an evidence based approach for the development of adjuvanted vaccines. *Curr Opin Immunol* **47**, 93-102, doi:10.1016/j.coi.2017.07.010 (2017).

8 Crepeaux, G. *et al.* Non-linear dose-response of aluminium hydroxide adjuvant particles: Selective low dose neurotoxicity. *Toxicology* **375**, 48-57, doi:10.1016/j.tox.2016.11.018 (2017).

9 Eisenbarth, S. C., Colegio, O. R., O'Connor, W., Sutterwala, F. S. & Flavell, R. A. Crucial role for the Nalp3 inflammasome in the immunostimulatory properties of aluminium adjuvants. *Nature* **453**, 1122-1126, doi:10.1038/nature06939 (2008).

10 Kool, M. *et al.* Cutting Edge: Alum Adjuvant Stimulates Inflammatory Dendritic Cells through Activation of the NALP3 Inflammasome. *The Journal of Immunology* **181**, 3755-3759, doi:10.4049/jimmunol.181.6.3755 (2008).

11 Li, H., Willingham, S. B., Ting, J. P. Y. & Re, F. Cutting Edge: Inflammasome Activation by Alum and Alum's Adjuvant Effect Are Mediated by NLRP3. *The Journal of Immunology* **181**, 17-21, doi:10.4049/jimmunol.181.1.17 (2008).

12 Marrack, P., McKee, A. S. & Munks, M. W. Towards an understanding of the adjuvant action of aluminium. *Nature reviews. Immunology* **9**, 287-293, doi:10.1038/nri2510 (2009).

13 Barber, G. N. STING: infection, inflammation and cancer. *Nature reviews. Immunology* **15**, 760-770, doi:10.1038/nri3921 (2015).

14 Luo, M. *et al.* A STING-activating nanovaccine for cancer immunotherapy. *Nature nanotechnology* **12**, 648-654, doi:10.1038/nnano.2017.52 (2017).

15 Corrales, L. *et al.* Direct Activation of STING in the Tumor Microenvironment Leads to Potent and Systemic Tumor Regression and Immunity. *Cell reports* **11**, 1018-1030, doi:10.1016/j.celrep.2015.04.031 (2015).

16 Del Giudice, G., Rappuoli, R. & Didierlaurent, A. M. Correlates of adjuvanticity: A review on adjuvants in licensed vaccines. *Semin Immunol* **39**, 14-21, doi:10.1016/j.smim.2018.05.001 (2018).

17 Sun, L., Wu, J., Du, F., Chen, X. & Chen, Z. J. Cyclic GMP-AMP synthase is a cytosolic DNA sensor that activates the type I interferon pathway. *Science* **339**, 786-791, doi:10.1126/science.1232458 (2013).

18 Ishikawa, H. & Barber, G. N. STING is an endoplasmic reticulum adaptor that facilitates innate immune signalling. *Nature* **455**, 674-678, doi:10.1038/nature07317 (2008).

19 Zhong, B. *et al.* The adaptor protein MITA links virus-sensing receptors to IRF3 transcription factor activation. *Immunity* **29**, 538-550, doi:10.1016/j.immuni.2008.09.003 (2008).

20 Sun, W. *et al.* ERIS, an endoplasmic reticulum IFN stimulator, activates innate immune signaling through dimerization. *Proc Natl Acad Sci U S A* **106**, 8653-8658, doi:10.1073/pnas.0900850106 (2009).

21 Tang, C. K. *et al.* The chemotherapeutic agent DMXAA as a unique IRF3-dependent type-2 vaccine adjuvant. *PloS one* **8**, e60038, doi:10.1371/journal.pone.0060038 (2013).

22 Blaauboer, S. M., Gabrielle, V. D. & Jin, L. MPYS/STING-mediated TNF-alpha, not type I IFN, is essential for the mucosal adjuvant activity of (3'-5')-cyclic-di-guanosine-monophosphate in vivo. *Journal of immunology* **192**, 492-502, doi:10.4049/jimmunol.1301812 (2014).

23 Li, X. D. *et al.* Pivotal roles of cGAS-cGAMP signaling in antiviral defense and immune adjuvant effects. *Science* **341**, 1390-1394, doi:10.1126/science.1244040 (2013).

24 Carroll, E. C. *et al.* The Vaccine Adjuvant Chitosan Promotes Cellular Immunity via DNA Sensor cGAS-STING-Dependent Induction of Type I Interferons. *Immunity* **44**, 597-608, doi:10.1016/j.immuni.2016.02.004 (2016).

25 Horning, K. J., Caito, S. W., Tipps, K. G., Bowman, A. B. & Aschner, M. Manganese Is Essential for Neuronal Health. *Annual review of nutrition* **35**, 71-108, doi:10.1146/annurev-nutr-071714-034419 (2015).

26 Kwakye, G. F., Paoliello, M. M., Mukhopadhyay, S., Bowman, A. B. & Aschner, M. Manganese-Induced Parkinsonism and Parkinson's Disease: Shared and Distinguishable Features. *International journal of environmental research and public health* **12**, 7519-7540, doi:10.3390/ijerph120707519 (2015).

27 Waldron, K. J., Rutherford, J. C., Ford, D. & Robinson, N. J. Metalloproteins and metal sensing. *Nature* **460**, 823-830, doi:10.1038/nature08300 (2009).

28 Wang, C. *et al.* Manganese Increases the Sensitivity of the cGAS-STING Pathway for Double-Stranded DNA and Is Required for the Host Defense against DNA Viruses. *Immunity* **48**, 675-687 e677, doi:10.1016/j.immuni.2018.03.017 (2018).

29 Gaidt, M. M. *et al.* The DNA Inflammasome in Human Myeloid Cells Is Initiated by a STING-Cell Death Program Upstream of NLRP3. *Cell* **171**, 1110-1124 e1118, doi:10.1016/j.cell.2017.09.039 (2017).

30 Swanson, K. V. *et al.* A noncanonical function of cGAMP in inflammasome priming and activation. *The Journal of experimental medicine* **214**, 3611-3626, doi:10.1084/jem.20171749 (2017).

31 Wree, A. *et al.* NLRP3 inflammasome driven liver injury and fibrosis: Roles of IL-17 and TNF in mice. *Hepatology*, doi:10.1002/hep.29523 (2017).

32 Amini, M. A. *et al.* Combining Tumor Microenvironment Modulating Nanoparticles with Doxorubicin to Enhance Chemotherapeutic Efficacy and Boost Antitumor Immunity. *J Natl Cancer Inst*, doi:10.1093/jnci/djy131 (2018).

33 Hussain, S. M. *et al.* The interaction of manganese nanoparticles with PC-12 cells induces dopamine depletion. *Toxicol Sci* **92**, 456-463, doi:10.1093/toxsci/kfl020 (2006).

34 Chen, H. *et al.* Optimisation of prime-boost immunization in mice using novel protein-based and recombinant vaccinia (Tiantan)-based HBV vaccine. *PloS one* **7**, e43730, doi:10.1371/journal.pone.0043730 (2012).

35 Lycke, N. Recent progress in mucosal vaccine development: potential and limitations. *Nature reviews. Immunology* **12**, 592-605, doi:10.1038/nri3251 (2012).

36 Cioncada, R. *et al.* Vaccine adjuvant MF59 promotes the intranodal differentiation of antigen-loaded and activated monocyte-derived dendritic cells. *PloS one* **12**, e0185843, doi:10.1371/journal.pone.0185843 (2017).

37 Langlet, C. *et al.* CD64 expression distinguishes monocyte-derived and conventional dendritic cells and reveals their distinct role during intramuscular immunization. *Journal of immunology* **188**, 1751-1760, doi:10.4049/jimmunol.1102744 (2012).

38 Ippagunta, S. K. *et al.* The inflammasome adaptor ASC regulates the function of adaptive immune cells by controlling Dock2-mediated Rac activation and actin polymerization. *Nature immunology* **12**, 1010-1016, doi:10.1038/ni.2095 (2011).

39 Kool, M. *et al.* Alum adjuvant boosts adaptive immunity by inducing uric acid and activating inflammatory dendritic cells. *The Journal of experimental medicine* **205**, 869-882, doi:10.1084/jem.20071087 (2008).

40 Oleszycka, E. *et al.* IL-1alpha and inflammasome-independent IL-1beta promote neutrophil infiltration following alum vaccination. *The FEBS journal* **283**, 9-24, doi:10.1111/febs.13546 (2016).

41 Glenny, A. T. Insoluble Precipitates in Diphtheria and Tetanus Immunization. *Br Med J* **2**, 244-245, doi:10.1136/bmj.2.3632.244 (1930).

42 Clapp, T., Munks, M. W., Trivedi, R., Kompella, U. B. & Braun, L. J. Freeze-thaw stress of Alhydrogel (R) alone is sufficient to reduce the immunogenicity of a recombinant hepatitis B vaccine containing native antigen. *Vaccine* **32**, 3765-3771, doi:10.1016/j.vaccine.2014.05.037 (2014).

43 Chen, D. *et al.* Characterization of the freeze sensitivity of a hepatitis B vaccine. *Hum Vaccin* **5**, 26-32 (2009).

44 Rigolet, M. *et al.* Clinical features in patients with long-lasting macrophagic myofasciitis. *Front Neurol* **5**, 230, doi:10.3389/fneur.2014.00230 (2014).

45 Maya, S., Prakash, T., Madhu, K. D. & Goli, D. Multifaceted effects of aluminium in neurodegenerative diseases: A review. *Biomedicine & pharmacotherapy = Biomedecine & pharmacotherapie* **83**, 746-754, doi:10.1016/j.biopha.2016.07.035 (2016).

46 Crisponi, G. *et al.* The meaning of aluminium exposure on human health and aluminium-related diseases. *Biomol Concepts* **4**, 77-87, doi:10.1515/bmc-2012-0045 (2013).

47 Baylor, N. W., Egan, W. & Richman, P. Aluminum salts in vaccines - US perspective (vol 20, pg S18, 2002). *Vaccine* **20**, 3428-3428 (2002).

48 May, J. C., Progar, J. J. & Chin, R. The Aluminum Content of Biological Products Containing Aluminum Adjuvants - Determination by Atomic-Absorption Spectrometry. *J Biol Stand* **12**, 175-183 (1984).

49 Lyons-Weiler, J. & Ricketson, R. Reconsideration of the immunotherapeutic pediatric safe dose levels of aluminum. *J Trace Elem Med Bio* **48**, 67-73 (2018).

50 Crepeaux, G. *et al.* Highly delayed systemic translocation of aluminum-based adjuvant in CD1 mice following intramuscular injections. *J Inorg Biochem* **152**, 199-205, doi:10.1016/j.jinorgbio.2015.07.004 (2015).

51 Gherardi, R. K. *et al.* Macrophagic myofasciitis lesions assess long-term persistence of vaccine-derived aluminium hydroxide in muscle. *Brain* **124**, 1821-1831, doi:10.1093/brain/124.9.1821 (2001).

52 Watad, A. *et al.* Autoimmune/inflammatory syndrome induced by adjuvants (ASIA) demonstrates distinct autoimmune and autoinflammatory disease associations according to the adjuvant subtype: Insights from an analysis of 500 cases. *Clin Immunol* **203**, 1-8, doi:10.1016/j.clim.2019.03.007 (2019).

53 Lyssiotis, C. A. & Kimmelman, A. C. Metabolic Interactions in the Tumor Microenvironment. *Trends Cell Biol* **27**, 863-875, doi:10.1016/j.tcb.2017.06.003 (2017).

54 Ben-Sasson, S. Z. *et al.* IL-1 acts directly on CD4 T cells to enhance their antigen-driven expansion and differentiation. *Proceedings of the National Academy of Sciences of the United States of America* **106**, 7119-7124, doi:10.1073/pnas.0902745106 (2009).

55 Wilson, N. S. *et al.* Inflammasome-dependent and -independent IL-18 production mediates immunity to the ISCOMATRIX adjuvant. *Journal of immunology* **192**, 3259-3268, doi:10.4049/jimmunol.1302011 (2014).

56 Williams, M. *et al.* in *Toxicological Profile for Manganese Agency for Toxic Substances and Disease Registry (ATSDR) Toxicological Profiles* (2012).

57 Davis, C. D., Zech, L. & Greger, J. L. Manganese metabolism in rats: an improved methodology for assessing gut endogenous losses. *Proc Soc Exp Biol Med* **202**, 103-108 (1993).

58 Britton, A. A. & Cotzias, G. C. Dependence of manganese turnover on intake. *Am J Physiol* **211**, 203-206, doi:10.1152/ajplegacy.1966.211.1.203 (1966).

59 Mahoney, J. P. & Small, W. J. Studies on manganese. 3. The biological half-life of radiomanganese in man and factors which affect this half-life. *J Clin Invest* **47**, 643-653, doi:10.1172/JCI105760 (1968).

Acknowledgements: We thank Ms. Liying Du, Drs Hongxia Lv, Guilan Li, Xiaochen Li from National Center for Protein Sciences at Peking University in Beijing, China, for assistance with FACS, protein purification and microscopy. We thank Drs. Yan Shi for OT-I and OT-II mice, Zhijian Chen for *Mavs*$^{-/-}$ mice, Rongbin Zhou for *Ifnar*$^{-/-}$ mice, Tadatsugu Taniguchi for *Irf3*$^{-/-}$ *Irf7*$^{-/-}$ mice, Vishva M. Dixit for *Aim2*$^{-/-}$, *Pycard*$^{-/-}$, *Nlrc4*$^{-/-}$ and *Nlrp3*$^{-/-}$ mice, Hongbing Shu, Yonghui Zhang, Wenjun Liu, Min Fang for viruses, Yonghui Zhang, Wenhui Li, Wenjie Tan, Changfa Fan for antigens. This work was supported by National Natural Science Foundation of China (31830022 and 81621001) and the Chinese Ministry of Science and Technology (2015CB943203).

Author contributions: R.Z., C.W. and Z.J. designed research; R.Z., C.W. and Y.G. performed the experiments, X.W., M.J., M.S., M.L., J.X. and Y.W. assisted in the experiments. R.Z., C.W. and Z.J. analyzed the data and wrote the manuscript.

Competing interests: The authors declare no competing interests.

Data and materials availability: All data supporting the findings of this study are available within the paper and its supplementary materials.

RNA-seq data have been deposited in Gene Expression Omnibus under accession no. GSE126586.

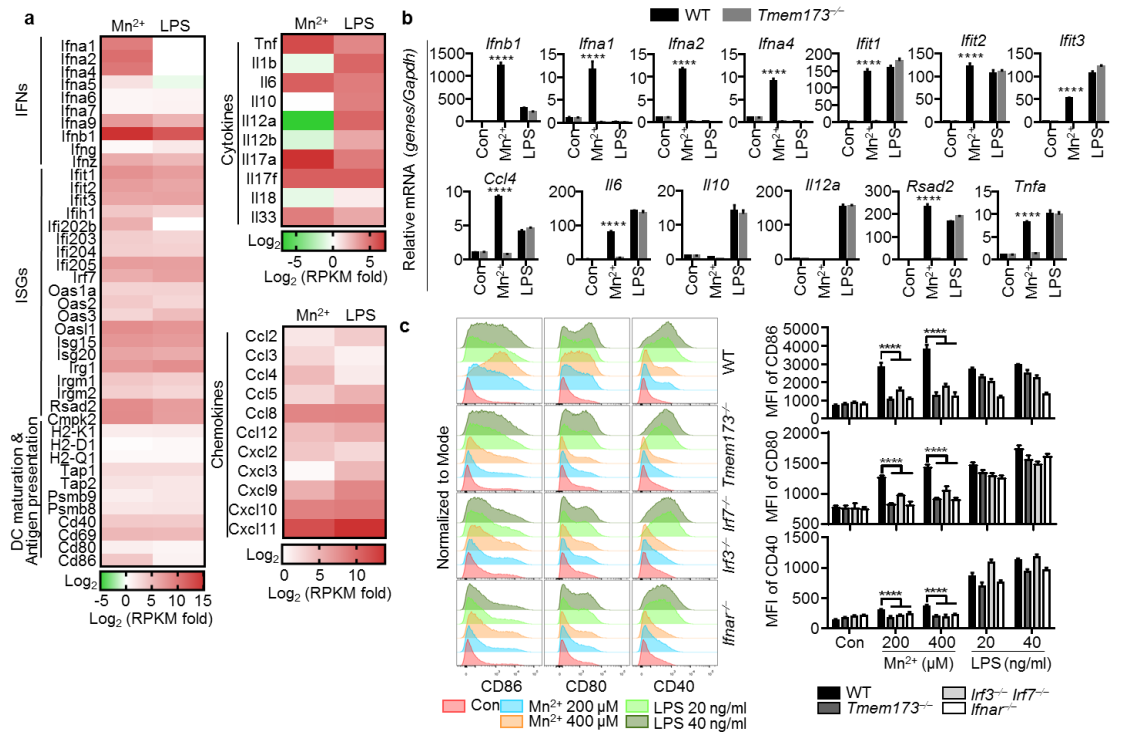

Fig. 1| Mn^{2+} Promotes DC Maturation via cGAS-STING Activation. a, Heatmap of RNA-seq analysis. BMDCs were untreated or treated with $MnCl_2$ (200 μM) or LPS (100 ng/ml) for 20 h. Heatmap was made by calculating log2 ((treated RPKM)/(control RPKM)). **b,** Quantitative RT-PCR analysis of the indicated gene expression in the WT and *Tmem173*$^{-/-}$ BMDCs treated with $MnCl_2$ (200 μM) or LPS (100 ng/ml) for 20 h. **c,** BMDCs from the WT, *Tmem173*$^{-/-}$, *Irf3*$^{-/-}$*Irf7*$^{-/-}$ or *Ifnar*$^{-/-}$ mice were treated with the indicated concentrations of $MnCl_2$ or LPS for 20 h. CD86, CD80 and CD40 expression was analyzed by FACS. One representative experiment of at least three independent experiments is shown, and each was done in triplicate. Error bars represent SEM; **b,** data were analyzed by two-way ANOVA; **c,** data were analyzed by an unpaired t test. ns, not significant; * $P < 0.05$; ** $P < 0.01$; *** $P < 0.001$; **** $P < 0.0001$.

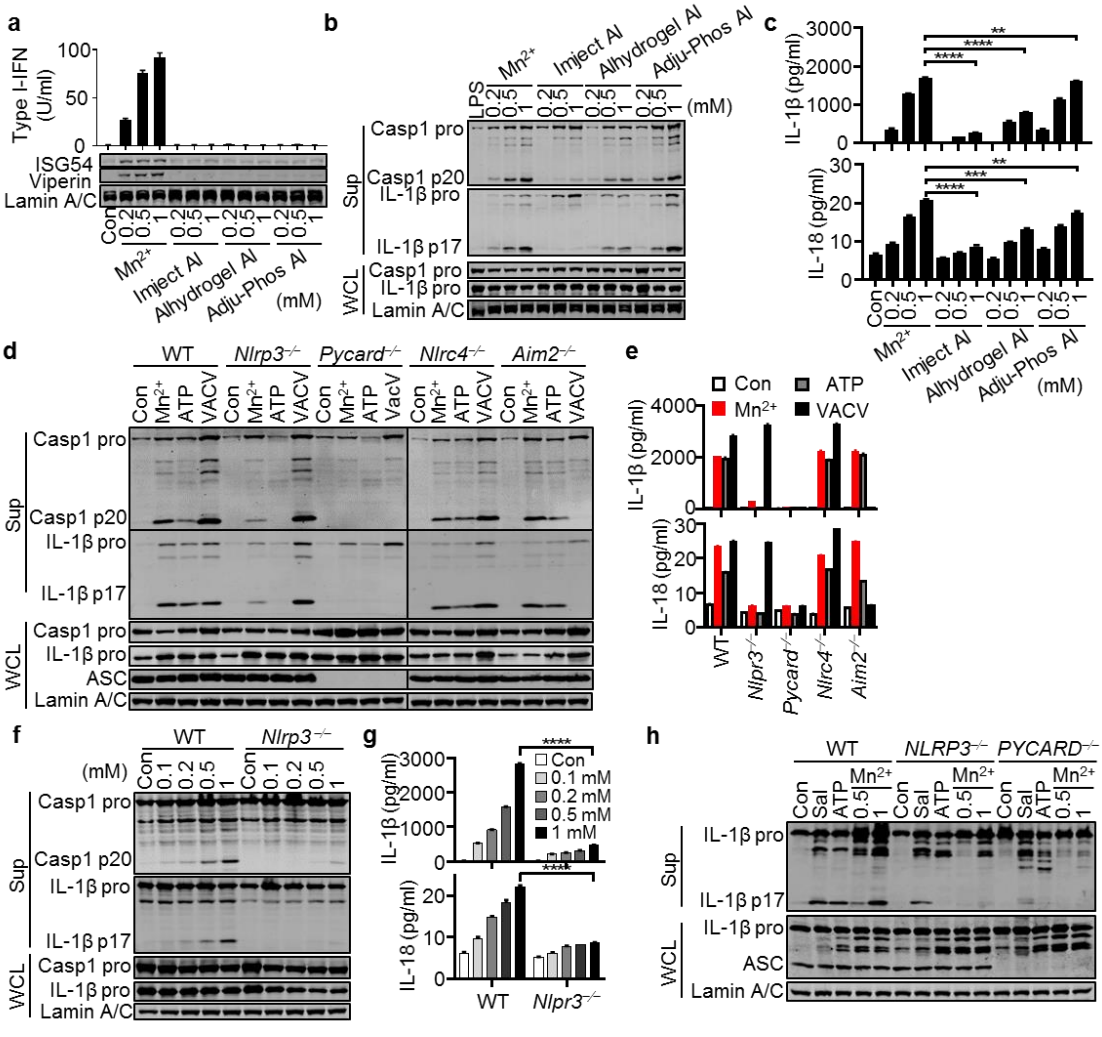

511

512 **Fig. 2| Mn^{2+} Activates NLRP3 Inflammasome. a,** Western blot (lower) and Type I-IFN

513 production analysis (upper) of mouse peritoneal macrophages treated with the indicated

514 concentrations of $MnCl_2$ or Aluminium salts (Imject® Alum, Alhydrogel® adjuvant 2%,

515 Adju-Phos® adjuvant) for 18 h. **b, c,** Western blot (**b**) and ELISA analysis (**c**) of inflammasome

516 activation of LPS-primed C57BL/6 peritoneal macrophages treated with the indicated

517 concentrations of $MnCl_2$ or Aluminium salts for 5 h. Supernatants (Sup) and whole cell lysates

518 (WCL) were analyzed by immunoblotting with the indicated antibodies. **d, e,** Western blot (**d**) and

519 ELISA analysis (**e**) of inflammasome activation of LPS-primed WT, *Nlrp3*$^{-/-}$, *Pycard*$^{-/-}$, *Nlrc4*$^{-/-}$

and *Aim2*$^{-/-}$ peritoneal macrophages treated with $MnCl_2$ (0.5 mM), ATP (5 mM) or VACV (MOI = 10). **f, g,** Western blot (**f**) and ELISA analysis (**g**) of inflammasome activation of LPS-primed WT and *Nlrp3*$^{-/-}$ peritoneal macrophages treated with the indicated concentrations of $MnCl_2$ for 5 h. **h,** Western blot analysis of inflammasome activation of LPS-primed THP1 cells treated with Salmonella (Sal, MOI = 10), ATP (5 mM) or $MnCl_2$ (0.5 and 1 mM). One representative experiment of at least three independent experiments is shown, and each was done in triplicate. Error bars represent SEM; **a, c, g,** data were analyzed by an unpaired t test. ns, not significant; * $P < 0.05$; ** $P < 0.01$; *** $P < 0.001$; **** $P < 0.0001$.

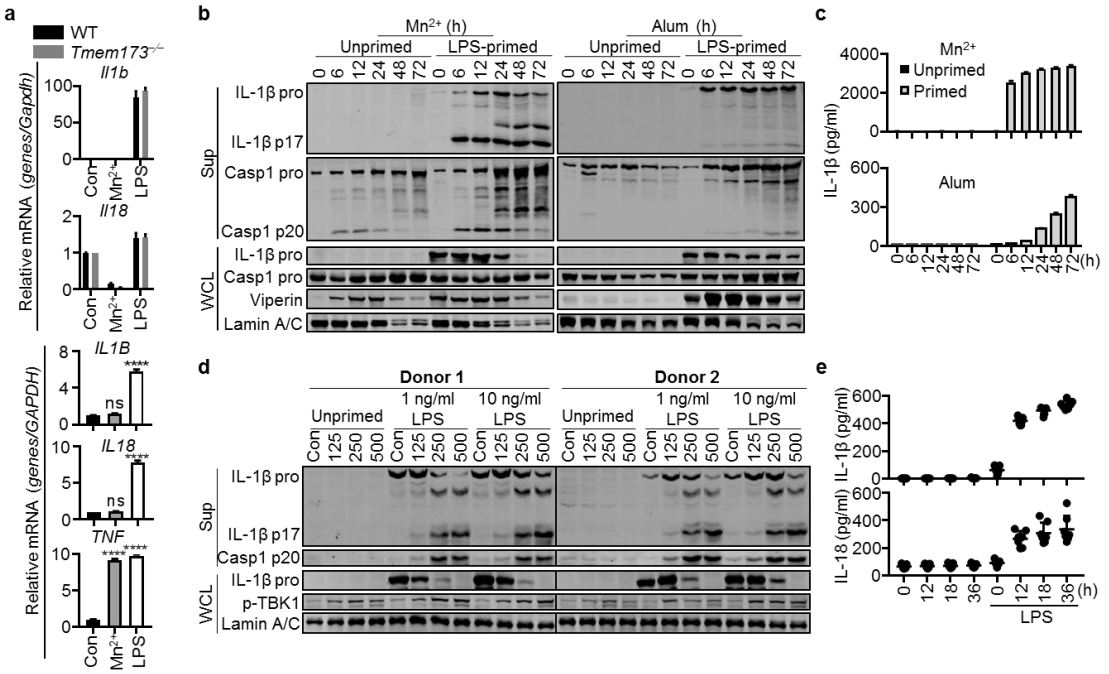

528

529 **Fig. 3| Mn^{2+} Activates Inflammasome without IL-1/-18 Production. a,** Quantitative RT-PCR

530 analysis of the indicated gene expression in the WT and *Tmem173*$^{-/-}$ BMDCs (upper) or human

531 Mo-DCs (lower) treated with $MnCl_2$ (200 μM) or LPS (100 ng/ml) for 20 h. **b, c,** Unprimed or

532 LPS-primed mouse peritoneal macrophages were treated with $MnCl_2$ (200 μM) or Alum (100

533 μg/ml) for the indicated times. Supernatants (Sup) and whole cell lysates (WCL) were analyzed by

534 immunoblotting with the indicated antibodies (**b**). IL-1β in supernatants was analyzed by ELISA

535 (**c**). **d, e,** Unprimed or LPS (1 ng/ml or 10 ng/ml)-primed human PBMCs were treated with $MnCl_2$

536 (200 μM) for the indicated times. Supernatants and whole cell lysates were analyzed by

537 immunoblotting with the indicated antibodies (**d**). Human IL-1β and IL-18 in supernatants were

538 analyzed by ELISA (**e**). One representative experiment of at least three independent experiments is

539 shown, and each was done in triplicate. Error bars represent SEM; **a,** data were analyzed by an

540 unpaired t test. ns, not significant; * $P < 0.05$; ** $P < 0.01$; *** $P < 0.001$; **** $P < 0.0001$.

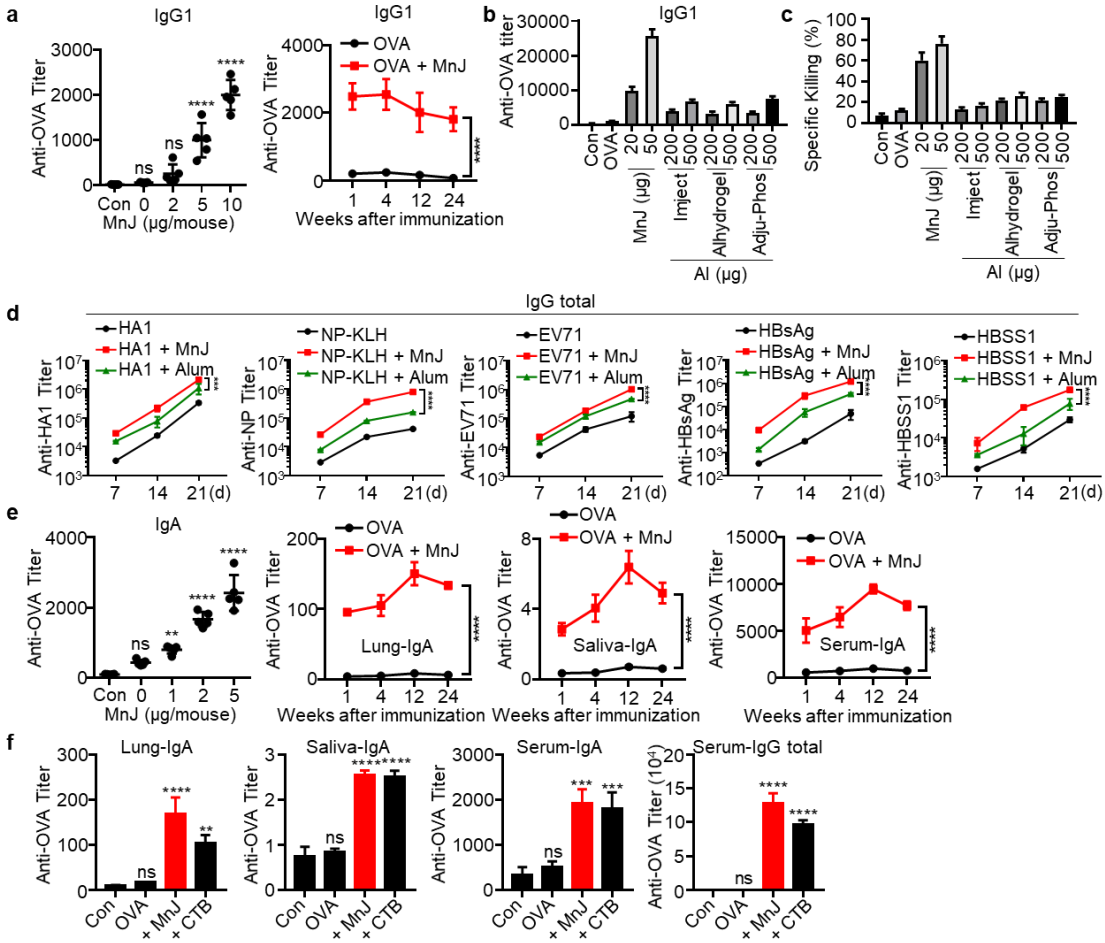

Fig. 4| MnJ Is A Potent Universal Adjuvant. a, The WT mice (C57BL/6) were immunized intramuscularly with PBS or OVA (10 μg) + MnJ (0, 2, 5 or 10 μg) on day 0, 7 and 14. Sera were collected on day 21 to measure OVA-specific IgG1 by ELISA (left, n = 5). Time course of OVA-specific IgG1 in sera from mice immunized intramuscularly with OVA (10 μg) + MnJ (10 μg) for three times (right, n = 3). **b, c,** The WT mice were immunized intramuscularly with PBS, OVA (10 μg), OVA (10 μg) + MnJ (5 μg) or OVA (10 μg) + indicated amounts of Aluminium salts. Sera were collected on day 21 to measure OVA-specific IgG1 by ELISA (**b**) (n = 4). OVA-specific cytotoxicity was measured on day 21 in an *in vivo* killing assay (**c**) (immunized on day 0, 7 and 14, n = 4). **d,** The WT mice were immunized intramuscularly with the indicated antigen (5 μg), antigen

(5 μg) + MnJ (10 μg) or antigen (5 μg) + Alum (1320 μg) on day 0, 7 and 14. Sera were collected on day 7, 14 and 21 to measure HA1, NP, EV71, HBsAg or HBSS1-specific IgG total (n = 3). **e,** The WT mice were immunized intranasally with PBS or OVA (10 μg) + MnJ (0, 1, 2 or 5 μg) on day 0, 7 and 14. Sera were collected on day 21 to measure OVA-specific IgA by ELISA (left, n = 5). Time course of OVA-specific IgA in BALF, saliva and serum as indicated from mice immunized intranasally with OVA (10 μg) + MnJ (5 μg) for three times (n = 3). **f,** OVA-specific IgA and IgG total were measured by ELISA on day 21 after immunization with OVA (10 μg), OVA (10 μg) + MnJ (5 μg) or OVA (10 μg) + CTB (10 μg) intranasally on day 0, 7 and 14 (n = 3). One representative experiment of at least three independent experiments is shown, and each was done in triplicate. Error bars represent SEM; **d,** data were analyzed by two-way ANOVA; **a, e, f,** data were analyzed by an unpaired t test. ns, not significant; * $P < 0.05$; ** $P < 0.01$; *** $P < 0.001$; **** $P < 0.0001$.

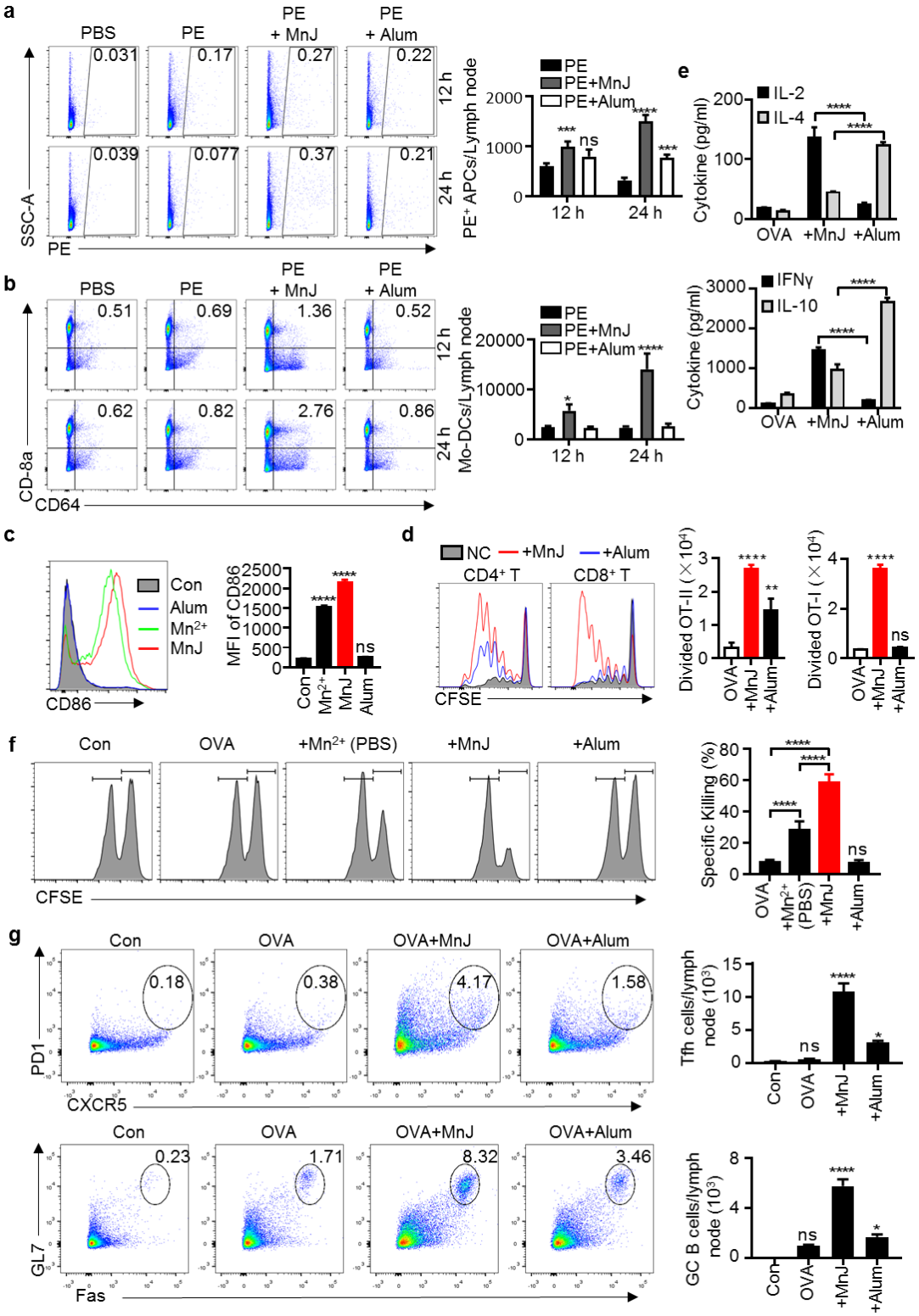

563

564 **Fig. 5| MnJ Promotes Antigen Presentation and T Cell Responses. a, b,** The WT mice were

565 immunized subcutaneously with PBS, Phycoerythrin (PE, 10 μg), PE (10 μg) + MnJ (20 μg) or PE

(10 μg) + Alum (200 μg). Inguinal lymph nodes were collected 12 or 24 h later (n = 3). Ratio and number of PE^+ APCs (**a**) and Mo-DCs (**b**) in dLN cells were analyzed by FACS. Live cells were identified by DAPI staining. Among live singlet cells, APCs were identified as the cell subset single or double positive for CD11c and F4/80. Among APCs, Mo-DCs were identified as $CD8a^+$ $CD64^+$ cells. **c,** BMDCs were treated with $MnCl_2$ (20 μg/ml), MnJ (20 μg/ml) or Alum (20 μg/ml) for 20 h. CD86 expression was analyzed by FACS. **d,** $CD45.1^+$ OT-I $CD8^+$ or OT-II $CD4^+$ T cells were labeled with CFSE and transferred to $CD45.2^+$ WT mice. These mice were then immunized with OVA (1 μg), OVA (1 μg) + MnJ (10 μg) or OVA (1 μg) + Alum (1320 μg). After 3 days, T cell proliferation was analyzed by FACS (n = 3). **e,** The WT mice were immunized intramuscularly with OVA (10 μg), OVA (10 μg) + MnJ (10 μg) or OVA (10 μg) + Alum (1320 μg) on day 0, 7 and 14. Splenocytes were collected on day 21, and stimulated with OVA (100 μg/ml). IL-2, IL-4, IFNγ and IL-10 secreted by T cells were measured by ELISA (n = 3). **f,** OVA-specific cytotoxicity was measured on day 21 in an *in vivo* killing assay (immunized on day 0, 7 and 14, n = 4). **g,** Numbers of Tfh or GC B cells in dLN from WT mice were analyzed by FACS. Live cells were identified by DAPI staining. Among live singlet cells, $CD4^+$ T cells were identified as the cell subset double positive for CD3 and CD4. Among $CD4^+$ T cells, Tfh cells were identified as $PD1^+$ $CXCR5^+$ cells. B cells were identified as the cell subset double positive for CD45 and B220. Among B cells, GC B cells were identified as Fas^+ $GL7^+$ cells. One representative experiment of at least three independent experiments is shown, and each was done in triplicate. Error bars represent SEM; **a, b, e,** data were analyzed by two-way ANOVA; **c, d, f, g,** data were analyzed by an unpaired t test. ns, not significant; * $P < 0.05$; ** $P < 0.01$; *** $P < 0.001$; **** $P < 0.0001$.

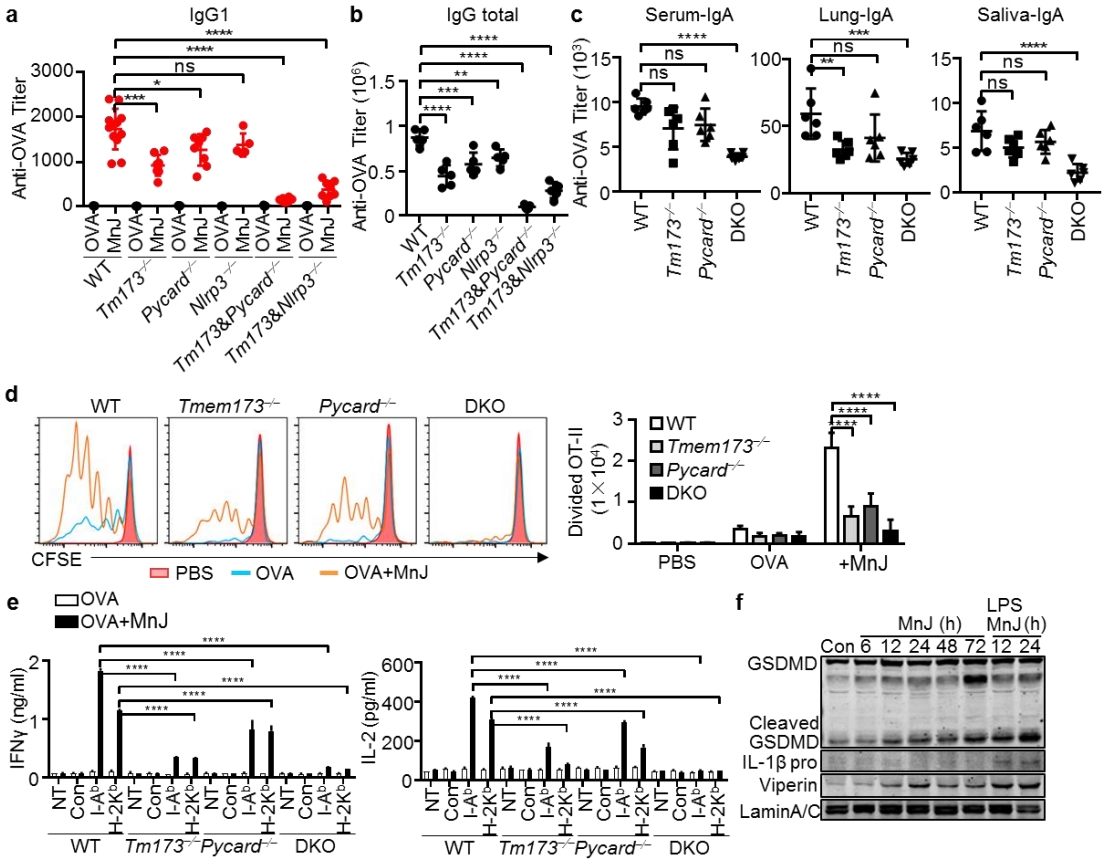

587

588 **Fig. 6| Both cGAS-STING and NLRP3 Inflammasome Contribute to Adjuvant Activity of**

589 **MnJ. a, b,** OVA-specific IgG1 (**a**) and IgG total (**b**) from the WT, *Tmem173*$^{-/-}$, *Pycard*$^{-/-}$, *Nlrp3*$^{-/-}$,

590 *Tmem173*$^{-/-}$*Pycard*$^{-/-}$ and *Tmem173*$^{-/-}$*Nlrp3*$^{-/-}$ mice were measured by ELISA on day 14 after

591 immunization with OVA (10 μg) or OVA (10 μg) + MnJ (10 μg) intramuscularly on day 0 and 7 (n >

592 5). **c,** OVA-specific IgA from the WT, *Tmem173*$^{-/-}$, *Pycard*$^{-/-}$ and *Tmem173*$^{-/-}$*Pycard*$^{-/-}$ DKO mice

593 was measured by ELISA on day 21 after immunization with OVA (10 μg) or OVA (10 μg) + MnJ

594 (5 μg) intranasally on day 0, 7 and 14 (n = 6). **d,** CD45.1^{+} OT-II CD4^{+} T cells were labeled with

595 CFSE and transferred to CD45.2^{+} WT, *Tmem173*$^{-/-}$, *Pycard*$^{-/-}$ and *Tmem173*$^{-/-}$*Pycard*$^{-/-}$ DKO mice.

596 These mice were then immunized with PBS, OVA (1 μg) or OVA (1 μg) + MnJ (10 μg). After 3

597 days, T cell proliferation was analyzed by FACS (n = 3). **e,** The WT, *Tmem173*$^{-/-}$, *Pycard*$^{-/-}$ and

598 *Tmem173*$^{-/-}$*Pycard*$^{-/-}$ DKO mice were immunized as (**a**). Splenocytes were collected on day 21,
599 and stimulated with OVA peptides. IFNγ and IL-2 secreted by T cells were measured by ELISA (n
600 = 3). **f,** The WT mice were immunized with MnJ (100 μg) or LPS (20 μg) + MnJ (100 μg)
601 intramuscularly for the indicated times. Lysates of draining lymph node cells were analyzed by
602 immunoblotting with the indicated antibodies. One representative experiment of at least three
603 independent experiments is shown, and each was done in triplicate. Error bars represent SEM; data
604 were analyzed by an unpaired t test. ns, not significant; * $P < 0.05$; ** $P < 0.01$; *** $P<0.001$; ****
605 $P < 0.0001$.

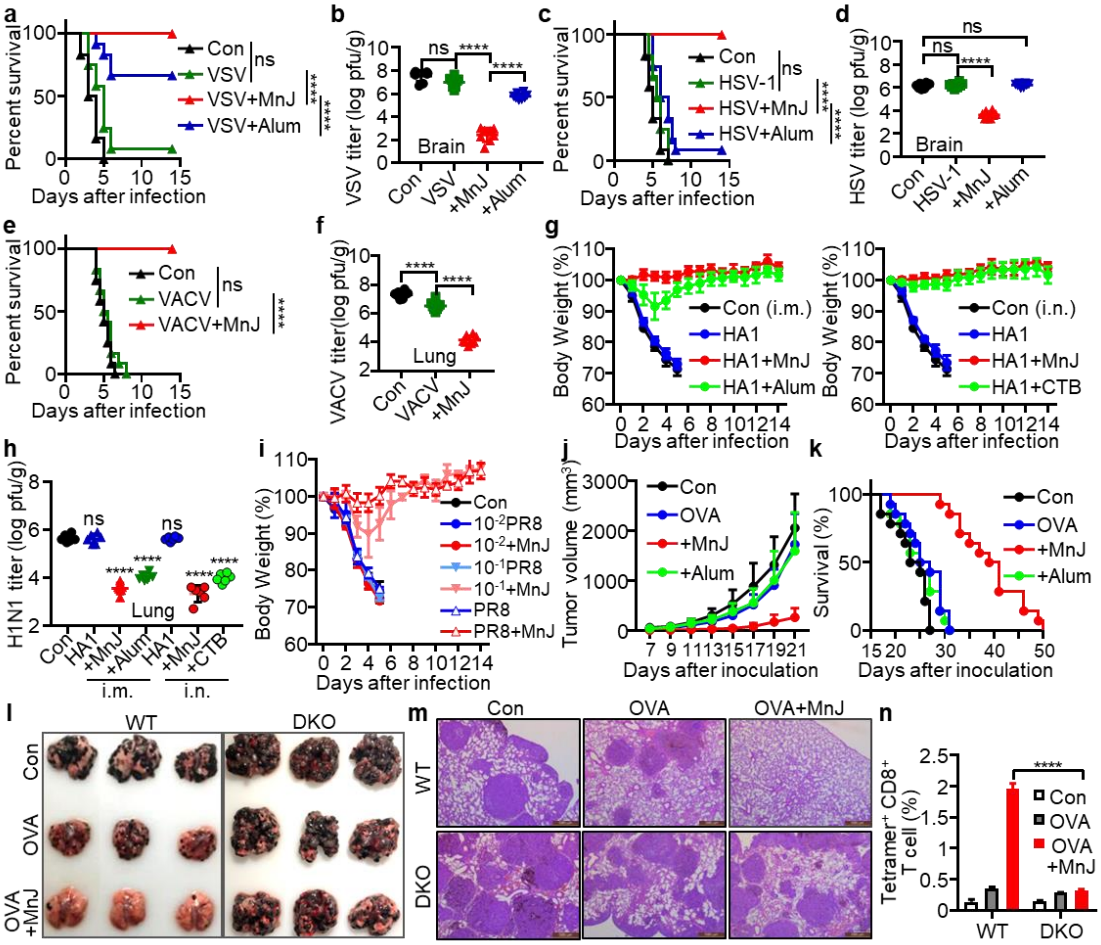

606

607 **Fig. 7| MnJ Is A Potent Adjuvant for Antiviral and Antitumor Vaccines. a, b,** The WT mice

608 were immunized intramuscularly with PBS, inactivated VSV (10^5 pfu), inactivated VSV (10^5 pfu)

609 + MnJ (10 μg) or inactivated VSV (10^5 pfu) + Alum (1320 μg) on day 0. On day 10, these mice

610 were infected intravenously with a lethal dose of VSV. The survival was monitored for 2 weeks (n

611 = 12) (**a**). Viral loads in brain were measured 5 days after infection (n = 8) (**b**). **c, d,** The WT mice

612 were immunized intramuscularly with PBS, inactivated HSV-1 (10^3 pfu), inactivated HSV-1 (10^3

613 pfu) + MnJ (10 μg) or inactivated HSV-1 (10^3 pfu) + Alum (1320 μg) on day 0. On day 10, these

614 mice were infected intraperitoneally with a lethal dose of HSV-1. The survival was monitored for 2

615 weeks (n = 12) (**c**). Viral loads in brain were measured 5 days after infection (n = 8) (**d**). **e, f,** The

WT mice were immunized intranasally with PBS, inactivated VACV (2×10^4 pfu) or inactivated VACV (2×10^4 pfu) + MnJ (5 μg) on day 0 and 7. On day 14, these mice were infected intranasally with a lethal dose of VACV. The survival was monitored for 2 weeks (n = 12) (**e**). Viral loads in lung were measured 5 days after infection (n = 8) (**f**). **g,** The WT mice were immunized intramuscularly (i.m.) with HA1 (5 μg), HA1 (5 μg) + MnJ (10 μg), HA1 (5 μg) + Alum (1320 μg) or intranasally (i.n.) with HA1 (5 μg), HA1 (5 μg) + MnJ (10 μg), or HA1 (5 μg) + CTB (10 μg) on day 0, 7 and 14. On day 21, these mice were infected intranasally with a lethal dose of PR8. The survival was monitored for 2 weeks (n = 10). **h,** The WT mice were immunized intranasally with PBS, inactivated PR8 (5×10^6 pfu), 10^{-1} PR8 (5×10^5 pfu) or 10^{-2} PR8 (5×10^4 pfu) with or without MnJ (5 μg) on day 0 and 7. On day 14, these mice were infected intranasally with a lethal dose of PR8. The body weight was recorded for 2 weeks (n = 3). **i,** Viral loads in lungs from mice in (**g**) were measured 5 days after infection (n = 6). **j, k,** The WT mice were immunized intramuscularly with PBS, OVA (10 μg), OVA (10 μg) + MnJ (20 μg) or OVA (10 μg) + Alum (1320 μg) on day 0, 7 and 14. On day 21, these mice were inoculated with B16-OVA-Fluc cells (3×10^5) subcutaneously. Tumor volume (**j**) was measured and survival (**k**) was monitored (n = 14). **l, m, n,** The WT and DKO mice were immunized intramuscularly with PBS, OVA (10 μg), or OVA (10 μg) + MnJ (20 μg) on day 0, 7 and 14. On day 21, these mice were inoculated with B16-F10-OVA (3×10^5) intravenously. Images (**l**) and HE staining (**m**) of lung tissues were recorded 20 days after inoculation (n = 6). The percentage of tetramer$^+$ CD8$^+$ T cells in spleens of these mice was analyzed by FACS on day 21 (n = 3) (**n**). One representative experiment of at least three independent experiments is shown, and each was done in triplicate. Error bars represent SEM;

637 **b, d, f, h, n,** data were analyzed by an unpaired t test; **a, c, e, k,** survival plot data were analyzed

638 with log-rank (Mantel–Cox) tests. ns, not significant; * $P < 0.05$; ** $P < 0.01$; *** $P<0.001$; **** P

639 < 0.0001.